ORGANIC LETTERS

2007
Vol. 9, No. 25
5215−5218

Steric Inhibition of π-Stacking: 1,3,6,8-Tetraarylpyrenes as Efficient Blue Emitters in Organic Light Emitting Diodes (OLEDs)

Jarugu Narasimha Moorthy,*,† Palani Natarajan,† Parthasarathy Venkatakrishnan,† Duo-Fong Huang,‡ and Tahsin J. Chow*,‡

Department of Chemistry, Indian Institute of Technology, Kanpur 208016, INDIA, and Institute of Chemistry, Academia Sinica, Taipei, Taiwan 115, Republic of China

moorthy@iitk.ac.in

Received September 24, 2007

ABSTRACT

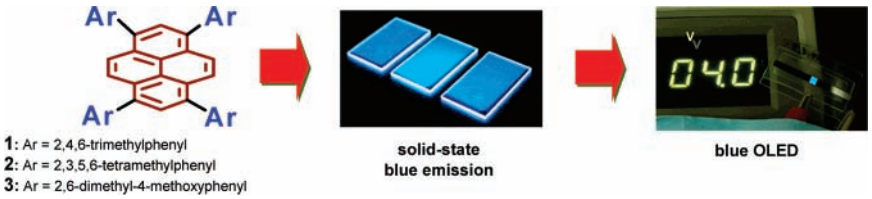

The sterically congested tetraarylpyrenes 1–3, which can be readily accessed by Suzuki coupling, exhibit no-aggregation (π-stacking) behavior in both solution and solid states. The indisposed tendency of 1–3 toward crystallization and their moderate molecular dimensions permit exploitation as blue light emitting materials in OLEDs with respectable device performances.

Flat aromatic molecules and linear π-conjugated systems are in general highly fluorescent[1] and find many applications in dyes,[2a] optical sensors,[2b] molecular electronics,[2c] nonlinear optics,[2d] light emitting diodes,[2e] photovoltaic cells,[2f] field-effect transistors,[2g] etc. However, a debilitating and well-known problem with these systems is that their emission in the solid state is effectively suppressed due to the formation of excimers via $\pi-\pi$ stacking.[3] For example, pyrene, a flat aromatic molecule, exhibits excellent fluorescent properties,[1] and the emission is pure blue to permit ready exploitation as an emissive material in organic light emitting diodes (OLEDs). However, its tendency to form dimers (excimers) in the excited state constitutes a severe impediment.[1] Several efforts[4] are currently underway to modulate the photophysical properties of pyrenes; for example, 1,3,6,8-tetraphenylpyrene (TPPy) is highly fluorescent (Φ ca. 0.9) in solution,[5] and the organic light emitting field-effect transistor devices (OLEFET) based on TPPy have been shown to exhibit electroluminescence (EL) with an external quantum efficiency of only 0.5% due to aggregation.[6]

Our recent results on the self-assembly of molecular modules based on sterically congested D_{2d}-symmetric bi-

† Indian Institute of Technology.
‡ Academia Sinica.

(1) Lakowicz, J. R. *Principles of Fluorescence Spectroscopy*; Plenum Press: New York, 1999.

(2) (a) Goeb, S.; Ziessel, R. *Org. Lett.* **2007**, *9*, 737. (b) Lee, S. H.; Kim, S. K.; Jung, J. H.; Kim, J. S. *J. Org. Chem.* **2005**, *70*, 9288. (c) Palma, M.; Levin, J.; Lemaur, V.; Liscio, A.; Palermo, V.; Cornil, J.; Geerts, Y.; Lehmann, M.; Samori, P. *Adv. Mater.* **2006**, *18*, 3313. (d) Chung, S. J.; Rumi, M.; Alain, V.; Barlow, S.; Perry, J. W.; Marder, S. R. *J. Am. Chem. Soc.* **2005**, *127*, 10844. (e) Yang, C.-H.; Guo, T.-F.; Sun, I.-W. *J. Lumin.* **2007**, *124*, 93. (f) Schmidt-Mende, L.; Fechtenkotter, A.; Mullen, K.; Moons, E.; Friend, R. H.; Mackenzie, J. D. *Science* **2001**, *293*, 1119. (g) Muccini, M. *Nat. Mater.* **2006**, *5*, 605.

(3) (a) Wurthner, F.; Thalacker, C.; Dieke, S.; Tschierske, C. *Chem.—Eur. J.* **2001**, *7*, 2245. (b) Jenekhe, S. A.; Osaheni, J. A. *Science* **1994**, *265*, 765.

(4) (a) Winnik, F. M. *Chem. Rev.* **1993**, *93*, 587. (b) Venkataramana, G.; Sankararaman, S. *Org. Lett.* **2006**, *8*, 2739. (c) de Halleux, V.; Calbert, J.-P.; Brocorens, P.; Cornil, J.; Declercq, J.-P.; Bredas, J. L.; Geerts, Y. *Adv. Funct. Mater.* **2004**, *14*, 649. (d) Rausch, D.; Lambert, C. *Org. Lett.* **2006**, *8*, 5037.

(5) Berlman, I. B. *J. Phys. Chem.* **1970**, *74*, 3085.

(6) Oyamada, T.; Uchiuzou, H.; Akiyama, S.; Oku, Y.; Shimoji, N.; Matsushige, K.; Sasabe, H.; Adachi, C. *J. Appl. Phys.* **2005**, *98*, 074506.

10.1021/ol7023136 CCC: $37.00
Published on Web 11/08/2007

mesityl scaffolds[7] prompted us to explore tetramesitylpyrene (**1**) and analogous duryl (**2**) and *p*-anisyl derivatives (**3**) as emissive materials. We surmised that the sterically congested 2,6-dimethylphenyl rings in these molecules would lie perpendicular to the plane of the central pyrene ring to prevent undesirable face-to-face π-stacking, so that self-quenching may be impeded to permit efficient emission in the solid state. In addition to the ready synthetic accessibility by Suzuki coupling, the bulky aryl rings in **1**−**3** were a priori anticipated to contribute to the improvement of thermal stability. We report herein that the pyrenes functionalized by sterically hindered aryl rings do not undergo close π-stacking leading to solid-state emission properties that parallel those in the solution state. Further, we show that such molecular systems lend themselves to application as pure-blue emissive materials in OLEDs.

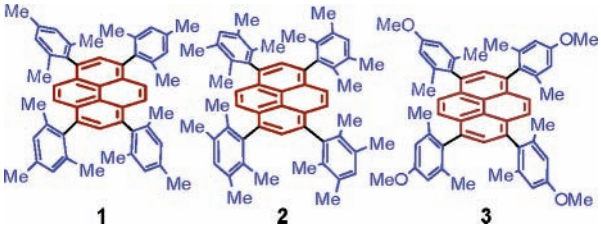

All the tetraarylpyrenes **1**−**3** were readily synthesized starting from 1,3,6,8-tetrabromopyrene. Suzuki coupling between the tetrabromopyrene and the corresponding arylboronic acids under Pd-catalyzed conditions afforded **1**−**3** in 75−80% isolated yields (cf. Supporting Information). The UV−vis absorption and fluorescence spectra of **1**−**3** in dichloromethane are presented in Figure 1. The absorption spectra

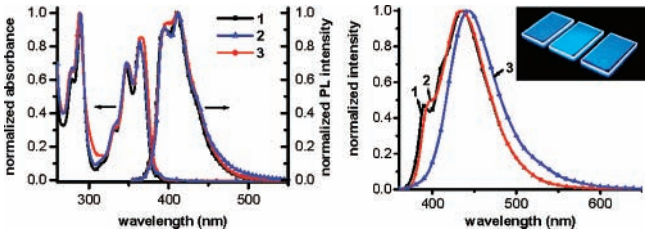

Figure 1. Left: UV−vis absorption and photoluminescence spectra of **1**−**3** in DCM. Right: The emission spectra of vacuum-deposited films of **1**−**3**. In the inset are shown the photographs of blue emission from the films of **1**−**3** (left→right).

reveal a vibronic feature that is characteristic of unsubstituted parent pyrene with short wavelength absorption maximum at ca. 289 nm. The long wavelength absorption maxima for **1**, **2**, and **3** occur at 363, 364, and 367 nm, respectively (Table 1), which points to only a marginal difference. The photoluminescence (PL) spectra for **1**−**3** in Figure 1 show that

Table 1. Absorption, PL, PL Quantum Yields, Electrochemical and Thermal Properties of Compounds **1**−**3**

	abs[a]	fl[a]						
sub	λ_{max} (nm)	λ_{max} soln (nm)	λ_{max} film (nm)	Φ_n[b] soln/film	band gap[c] (eV)	HOMO/LUMO[c] (eV)	T_m[e] (°C)	T_d[f] (°C)
1	363	411	435	0.28 0.30	3.19	5.8(5.9)[d] 2.6	242	302
2	364	412	434	0.33 0.24	3.18	5.8(5.9)[d] 2.6	291	367
3	367	411	442	0.38 0.44	3.16	5.8(5.9)[d] 2.6	249	392

[a] In DCM (ca. 1×10^{-6} M). [b] Using 9,10-diphenylanthracene as a standard; $\lambda_{ex} = 330$ nm. [c] See text. [d] Vertical ionization potential, as determined by photoelectron spectroscopy. [e] By DSC. [f] By TGA.

their emission maxima lie in the region between 400 and 450 nm. All pyrenes **1**−**3** emit bright blue fluorescence even at concentrations as low as 10^{-6} M. There occurs ca. 20−30 nm red shift in their emission maxima as compared to those in the solution state; this difference may be due to solvation effects and lack thereof in the films. Otherwise, the absence of palpable red-shifted emission in all **1**−**3** attests to the fact that the molecules do not aggregate in the solid state to form excimers, which is also evidenced from X-ray crystal structure determination of one of the pyrenes (i.e., tetramesitylpyrene **1**; vide infra). The PL quantum yields of **1**−**3** in cyclohexane solution were found to vary from 0.28 to 0.38 (Table 1).[8] Remarkably, the quantum yields for vacuum-deposited films were found to be in the range of 0.24−0.44, which closely parallel those observed in the solution state.

In order to examine the molecular organization in the solid state, the crystallization of tetramesitylpyrene **1**, a representative case, was attempted in various solvents. While the compound fell out as an amorphous powder in several solvents, crystals suitable for diffraction studies were obtained from solvents such as chloroform + ethyl acetate, benzene, and mesitylene. However, the crystals were found to decay once they were removed from the mother liquor, which suggests the incorporation of guest molecules in the crystal lattice. Indeed, the X-ray crystal structure determined for **1** at 100 K revealed the presence of chloroform and highly disordered ethyl acetate in the crystal lattice (cf. Supporting Information); it is noteworthy that the crystals lost their crystallinity and turned amorphous with slow exclusion of the lattice-included solvent. The crystals in the case of **1** corresponded to triclinic crystal system ($P\bar{1}$). As shown in Figure 2, the central pyrene ring and the mesityl rings lie almost orthogonally with angles between the pyrene and mesitylene rings falling in the range of 86.2−88.2°. The crystal packing, also shown in Figure 2, shows that the molecules are off-set with respect to each other in perpen-

(7) (a) Moorthy, J. N.; Natarajan, R.; Venugopalan, P. *J. Org. Chem.* **2005**, *70*, 8568. (b) Natarajan, R.; Savitha, G.; Moorthy, J. N. *Cryst. Growth Des.* **2005**, *5*, 69. (c) Natarajan, R.; Savitha, G.; Dominiak, P.; Wozniak, K.; Moorthy, J. N. *Angew. Chem., Int. Ed.* **2005**, *44*, 2115.

(8) The quantum yield for unsubstituted parent pyrene in cyclohexane is 0.32. See: Berlman, I. B. *Handbook of Fluorescence Spectra of Aromatic Molecules*; Academic Press: New York, 1971.

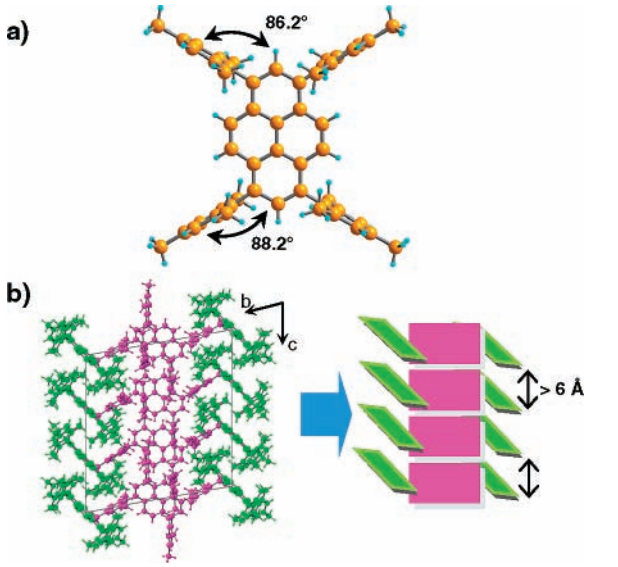

Figure 2. (a) A perspective drawing of the molecular structure of one of the three molecules in the asymmetric unit cell of **1**; the structures of the other two are similar. (b) The crystal packing diagram of **1** viewed down *a*-axis; the guest chloroform and ethyl acetate molecules have been removed for clarity. The green and magenta colors signify the perpendicular and planar arrangement of molecules, respectively. The orthogonal arrangement of the molecules is shown by a cartoon drawing.

dicular columns; the distance between the planes of the inclined pyrene central rings is >6 Å (cf. Supporting Information).

Electrochemically, all pyrenes **1**−**3** were found to exhibit a reversible one-electron oxidation within the observable potential window (cf. Supporting Information). While the HOMOs were derived from their oxidation potentials, the LUMOs were calculated by subtracting the corresponding optical band gap energies from the HOMO values. The HOMOs and LUMOs for **1**−**3** vary from 5.75 to 5.80 eV and 2.56 to 2.62 eV, respectively (cf. Table 1). The HOMOs determined via cyclic voltammetry were found to be comparable to the vertical ionization potentials determined by photoelectron spectroscopy (5.9 eV). Thermal properties of **1**−**3** were gauged by thermogravimetric analysis (TGA) and differential scanning calorimetry (DSC) (cf. Table 1 and Supporting Information). The pyrenes **1**−**3** were found to exhibit decomposition temperatures (T_d) above 300 °C, while a broad endothermic melting transition (T_m) was found above 240 °C; indeed, the thermal properties of **1**−**3** are comparable to and higher than those reported so far for simple pyrene analogues; for example, T_m(1,3,6,8-tetrakis(*p*-methoxyphenyl)pyrene) = 263 °C.[4c]

The functional behavior of **1**−**3** as emitting materials in OLEDs was investigated by fabricating devices for capturing electroluminescence (EL). All **1**−**3** were readily sublimed under vacuum (10^{-6} Torr) to construct multilayer devices. The common device configuration was ITO/NPB (400 Å)/**1**−**3** (100 Å)/TPBI (400 Å)/LiF (10 Å)/Al (1500 Å), where ITO (indium tin oxide) was the anode, NPB (*N*,*N*′-bis(naphthalen-1-yl)-*N*,*N*′-bis(phenyl)benzidine) served as a hole-transporting layer, **1**/**2**/**3** as an emitting layer, TPBI (2,2′,2″-(1,3,5-benzinetriyl)tris(1-phenyl-1*H*-benzimidazole) as an electron-transporting layer, and LiF:Al as the composite cathode. The above non-doped devices constructed for **1**−**3** showed a bright *blue* electroluminescence (cf. Figure 3) at a turn-on voltage of 4.0−5.0 V (Table 2). The

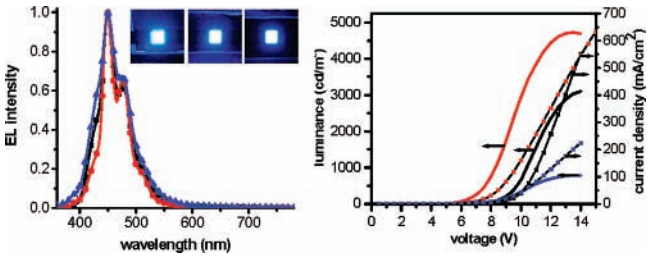

Figure 3. The EL spectrum (left) and the *I*−*V*−*L* curves (right) for **1** (black), **2** (blue), and **3** (red). The inset shows photographs of the bright blue emission captured from the devices for **1**−**3** (left→right).

Table 2. EL Data for the Devices ITO/NPB (400 Å)/**1** or **2** or **3** (100 Å)/TPBI (400 Å)/LiF (10 Å)/Al (1500 Å)

sub	V_{on}[a]	η_{ex}[b] (V)	η_p[c]	η_1[d] (V)	λ_{max} EL	L_{100}[e] (V)	L_{max}[f]	CIE *x*, *y*
1	5.0	2.6	0.61	2.2	450	1326	3106	0.15
		7.5		7.5		10.7		0.10
2	5.0	1.01	0.19	0.9	448	412	696	0.14
		8.0		8.0		10.0		0.08
3	4.0	3.26	1.03	2.7	448	2058	4730	0.14
		6.5		6.5		9.25		0.09

[a] Turn-on voltage (V). [b] External quantum efficiency (%). [c] Power efficiency (lm/W) @20 mA/cm². [d] Luminance efficiency (cd/A). [e] Luminance (cd/m²) @100 mA/cm². [f] Maximum luminance (cd/m²).

luminance and external quantum efficiencies of the device constructed for **1** were 1.85 cd/A and 2.2%, respectively, at a current density of 20 mA/cm² (9.48 V). The maximum luminance achieved was 3106 cd/m². In contrast, the device constructed for **3** exhibited much better performance, yielding a maximum external quantum efficiency of ca. 3.3% at 6.5 V. The maximum luminance efficiency achieved was 2.7 cd/A at a current density of 5.25 mA/cm² (6.5 V) with a maximum luminance of 4730 cd/m². Intriguingly, the device performances for **2** were poorer, suggesting the fact that marginal structural variations lead to drastic differences in the performances of the solid-state devices.

As mentioned at the outset, our objective in installing 2,6-dimethylaryl rings at four corners of the flat pyrene ring perpendicularly is to conserve optical absorption and emission properties of parent pyrene and to also impede molecular aggregation via face-to-face π-stacking. As is evident from absorption spectra for **1**−**3** and the crystal structure determined for representative pyrene **1**, the molecules do not

undergo π-stacking. Understandably, the rigid structures with orthogonal planes should face molecular packing problems such that they crystallize out only in the presence of guest molecules, which get included in the crystal lattice; this concept has been exploited by Aoyama and co-workers[9] to develop organic hydrogen-bonded porous materials. A consequence of this is that such compounds fall out as amorphous powders in the absence of suitable guest molecules. The amorphous property is a highly desirable prerequisite for application of an organic compound as a functional material in OLEDs.[10] The amorphous nature permits uniform pin-hole-free deposition of thin films in addition to the fact the indisposed tendency of the molecules toward crystallization (without guests) obviates creation of defect sites at which the excitons are nonradiatively quenched; there is an intimate relationship between the crystallinity of the film and device performance.[11] The fact that the solid-state fluorescence quantum yields parallel those of the solution state is suggestive of similar emissive behavior in both media.

The 4-fold substitution by 2,6-dimethylaryl rings in **1**−**3** considerably improves their morphology as well as thermal stability, as revealed from their thermal decomposition temperatures (cf. Table 1); for example, T_d for **3** is ca. 392 °C. Further, the energy gap between the HOMO and LUMO of **1**−**3** is as high as ca. 3.2 eV, which is very advantageous from the point of view of their application as host materials for Förster-type energy transfer in OLEDs; indeed, only a limited number of wide gap blue emitting materials are currently available as hosts in light emitting devices.[12] Thus, red, green, and white lights may be conveniently derived from blue emitting materials with wide band gap energy via a downhill energy transfer to generate full color displays, which constitutes an ultimate objective of the contemporary research on OLEDs.[13]

Pyrene-based triarylamines,[14] oligoquinolines,[15] quinoxalines,[16] fluorenes,[17] oligothiophenes,[18] and octavinylsilsesquioxane,[19] etc. have been reported in the literature as hole-transporting, emitting, and host materials. The moderate molecular size and rigid non-coplanar aromatic planes intrinsic to **1**−**3**, which retard crystallization, permit sublimation without any decomposition in the vacuum chamber. Thus, the vacuum-sublimed devices constructed for **1**−**3** exhibit bright blue light emission with λ_{max} at ca. 450 nm. It is noteworthy that the maximum external quantum efficiency achieved for the non-doped device fabricated for **3** is 3.3%; this value is comparable to commonly used blue emitting materials based on spirobifluorene (3.2 cd/A),[20a] diarylanthracenes (2.6−3.0 cd/A),[20b,c] diphenylvinylbiphenyls (1.78 cd/A),[20d] biaryls (4.0 cd/A),[20e] etc. The maximum luminance efficiency of 2.7 cd/A achieved in the case of **3** underscores the fact that the attachment of sterically hindered substituents to the pyrene does indeed lead to suppression of face-to-face aggregation. It is instructive to note that the emission is pure blue according to the CIE coordinates. The observed external quantum yield and luminance efficiencies for **1**−**3** are respectably high, which warrants further investigations of analogous derivatives to afford materials with improved properties.

In conclusion, we have shown that sterically congested tetraarylpyrenes **1**−**3** can be readily accessed via facile Suzuki coupling and that the 4-fold functionalization manifests in steric inhibition of molecular aggregation in both solution (UV−vis and fluorescence) and solid states (photoluminescence and crystal packing). The arene units so attached impart thermal stability and noncrystalline property to permit the potential of **1**−**3** as emissive materials in OLEDs to be readily explored. The devices fabricated for **1**−**3** lead to *pure blue* electroluminescence with respectable device performances.

Acknowledgment. J.N.M. is thankful to DST, India, for funding. P.N. is grateful to UGC for a research fellowship. Dr. P. Venugopalan, Chandigarh, is gratefully acknowledged for the help with structure refinement.

Supporting Information Available: Experimental procedures, spectral data (^{1}H and ^{13}C NMR), X-ray structure determination details, and cif file. This material is available free of charge via the Internet at http://pubs.acs.org.

OL7023136

(9) Endo, K.; Ezuhara, T.; Koyanagi, M.; Masuda, H.; Aoyama, Y. *J. Am. Chem. Soc.* **1997**, *119*, 499.
(10) Shirota, Y. *J. Mater. Chem.* **2000**, *10*, 1.
(11) Joswick, M. D.; Cambell, I. H.; Barashkov, N. N.; Ferraris, J. P. *J. Appl. Phys.* **1996**, *80*, 2883.
(12) (a) Lee, M. T.; Chen, H. H.; Liao, C. H.; Tsai, C. H; Chen, C. H. *Appl. Phys. Lett.* **2004**, *85*, 3301. (b) Shi, J.; Tang, C. W. *Appl. Phys. Lett.* **2002**, *80*, 3201. (c) Shen, W. J.; Dodda, R.; Wu, C. C.; Wu, F. I.; Liu, T. H.; Chen, H. H.; Chen, C. H.; Shu, C. F. *Chem. Mater.* **2004**, *16*, 930. (d) Hosokawa, C.; Tokailin, H.; Higashi, H.; Kusumoto, T. *J. Appl. Phys.* **1995**, *78*, 5831.
(13) Kido, J.; Hongawa, K.; Nagai, K. *Macromol. Symp.* **1994**, *84*, 81.
(14) Thomas, K. R. J.; Velusamy, M.; Lin, J. T.; Chuen, C. H.; Tao, Y. T. *J. Mater. Chem.* **2005**, *15*, 4453.
(15) Hancock, J. M.; Gifford, A. P.; Tonzola, C. J.; Jenekhe, S. A. *J. Phys. Chem. C* **2007**, *111*, 6875.
(16) Huang, T.-H.; Whang, W. T.; Zheng, H. G.; Lin, J. T. *J. Chin. Chem. Soc.* **2006**, *53*, 223.
(17) (a) Tang, C.; Liu, F.; Xia, Y.-J.; Xie, L.-H.; Wei, A.; Li, S.-B.; Fan, Q.-L.; Huang, W. *J. Mater. Chem.* **2006**, *16*, 4074. (b) Tao, S. T.; Peng, Z. K.; Zhang, X. H.; Wang, P. F.; Lee, C.-S.; Lee, S.-T. *Adv. Funct. Mater.* **2005**, *15*, 1716.
(18) Otsubo, T.; Aso, Y.; Takimiya, K. *J. Mater. Chem.* **2002**, *12*, 2565.
(19) Lo, M. Y.; Zhen, C.; Lauters, M.; Jabbour, G. E.; Sellinger, A. *J. Am. Chem. Soc.* **2007**, *129*, 5808.
(20) (a) Kim, Y.-H.; Shin, D.-C.; Kim, S.-H.; Ko, C.-H.; Yu, H.-S.; Chae, Y.-S.; Kwon, S.-K. *Adv. Mater.* **2001**, *13*, 1690. (b) Kim, Y.-H.; Jeong, H.-C.; Kim, S.-H.; Yang, K.; Kwon, S.-K. *Adv. Funct. Mater.* **2005**, *15*, 1799. (c) Tao, S. L.; Hong, Z. R.; Peng, Z. K.; Ju, W. G.; Zhang, X. H.; Wang, P. H.; Wu, S. K.; Lee, S. T. *Chem. Phys. Lett.* **2004**, *397*, 1. (d) Xie, W.; Hou, J.; Liu, S. *Semicond. Sci. Technol.* **2003**, *18*, L42. (e) Shih, H.-T.; Lin, C.-H.; Shih, H.-H.; Cheng, C.-H. *Adv. Mater.* **2002**, *14*, 1409.